Pure Appl. Chem., Vol. 80, No. 9, pp. 1909–1918, 2008.
doi:10.1351/pac200880091909

Self-organized nanoarrays: Plasma-related controls*

Kostya (Ken) Ostrikov[1,2,‡], Igor Levchenko[1], and Shuyan Xu[3]

[1]Plasma Nanoscience, School of Physics, The University of Sydney, Sydney, NSW 2006, Australia; [2]CSIRO Materials Science and Engineering, West Lindfield, NSW 2070, Australia; [3]Plasma Sources and Applications Center, NIE and Institute of Advanced Studies, Nanyang Technological University, 637616, Singapore

Abstract: The paper presents an investigation of self-organizational and -assembly processes of nanostructure growth on surfaces exposed to low-temperature plasmas. We have considered three main growth stages—initial, or sub-monolayer growth stage, separate nanostructure growth stage, and array growth stages with the characteristic sizes of several nm, several tens of nm, and several hundreds of nm, respectively, and have demonstrated, by the experimental data and hybrid multiscale numerical simulations, that the plasma parameters can strongly influence the surface processes and hence the kinetics of self-organization and -assembly. Our results show that plasma-controlled self-organization is a promising way to assemble large regular arrays of nanostructures.

Keywords: quantum dots; carbon nanotubes; nanowalls; self-assembly; self-organization; low-temperature plasma.

INTRODUCTION

Modern nanotechnology requires the rapid development of sophisticated methods for the formation of various nanostructures with different geometric, physical, chemical, structural, etc. characteristics [1,2], such as nanotubes [3,4], quantum dots (QDs), nanotips [5], and nanowalls [6] of various materials including carbon, aluminum nitride, silicon carbide, and others. The elemental composition (including internal core/shell and core/shell/undershell structures) and geometrical characteristics have always been considered to be the key parameters responsible for the fundamental properties of specific nanostructures [7]; nevertheless, large-scale ordering, by nanostructure size and position, is very important in some applications.

From the self-assembly and -organization point of view, the methods of nanostructure synthesis based on low-temperature plasmas and ion beams appear to be more attractive than the methods based completely on neutral (atom and molecular) fluxes [8,9]. The presence of an electrical potential on the substrate, and hence strong electric fields between the surface of the substrate, nanostructures, and plasma bulk, enables an effective control of the growth conditions of nanostructure arrays developing on the surface [10].

Plasma-based nanofabrication methods include but are not limited to plasma-enhanced chemical vapor deposition [11,12], microwave plasma deposition [13], plasma-assisted magnetron sputtering [14–16], and laser ablation [17,18]. These techniques possess significant advantages, as compared to

*Paper based on a presentation at the 18th International Symposium on Plasma Chemistry (ISPC-18), 26–31 August 2007, Kyoto, Japan. Other presentations are published in this issue, pp. 1883–2023.

‡Corresponding author: E-mail: Kostya.Ostrikov@csiro.au

processes based on the deposition of neutral flux [19] (in the nanostructure alignment [20], treatment uniformity [21,22], and size distribution [23]) due to the strong influence of the electric [24,25] and magnetic [26] fields on the growth conditions. Reducing the characteristic size of nano-objects does not favor the use of template-based techniques; as a result, there is a strong interest in self-organization which also favors the use of plasma processes, as there are more possibilities for the process control [19,27].

In this work we mainly concentrate on the self-organizational phenomena during nanostructure formation in low-temperature plasma environments. We analyze the three main stages (initial nucleation, separate nanostructure growth, and array development) of the nanoarray formation by experimentally obtained data, along with hybrid numerical multiscale simulations. It will be demonstrated that the growth process, self-assembly, and self-organization in the large arrays of nanostructures can be effectively controlled in the plasma-based deposition process. We show that the initial seed pattern formation on the surface, nanostructure crystallization, and nanostructure array reorganization involve processes which can be effectively controlled by changing the plasma parameters.

SELF-ORGANIZATION AND DEVELOPMENT OF NANOARRAYS

The process of nanoarray (e.g., QDs, nanotubes, nanotips, nanowalls, etc.) formation may be conditionally divided into the three main stages called the initial (sub-monolayer) stage involving nucleation of ultra-small (up to 1 nm) nanoclusters; individual nanostructure growth stage which consists in the growth of nano-objects of several nm size without mutual influence; and, finally, development stage when nano-objects interact with each other. In this paper we do not examine the various aspects of the growth at different stages; instead, we focus on the self-organization aspects at each stage. More precisely, our task is to point out the specific physical processes that (a) can be effectively controlled via the plasma parameters; and (b) strongly influence the surface processes involved in the nanostructuring/nanoarray formation.

Presently, a number of different techniques are used for nanoarray formation; in general, they can be divided into two main groups, namely, template-involving and self-organization-based methods. The application of template-involving techniques is strongly restricted by the template feature sizes which represent a fundamental restriction [28]. On the other hand, the methods based on self-organization have no such restriction. In a sense, these methods are “up-restricted”, i.e., they cannot be used for large nanostructures; however, with the characteristic sizes of nanostructure continuously decreasing, self-organization-based methods acquire a growing importance.

A general examination of the physics involved in nanoarray formation shows that there are two main parameters that appear to be both plasma-controllable and simultaneously important for the self-organization of the nanoarrays. These parameters are the surface temperature and the surface diffusion activation energy. Thus, our specific aim is to demonstrate how and to what extent the temperature and surface diffusion activation energy, being controlled by the plasma-related parameters, affect the kinetics of surface processes important for self-organization.

SELF-ORGANIZATION AND -ASSEMBLY AT INITIAL STAGES OF DEPOSITION

Here we consider an initial, or sub-monolayer growth stage of the nanoarray formation, with the characteristic size of nano-objects up to 1 nm (thus, we consider nano-objects, or nanoclusters, consisting of a small number of atoms, up to 20–25). Present-day capabilities of plasma-based nanofabrication are insufficient to investigate this process experimentally, thus, numerical simulation is an effective tool which enables detailed analysis of the processes involved. At this stage, the process kinetics is mainly determined by the kinetics of the interaction of adsorbed atoms (adatoms) with the substrate surface and nano-objects [29,30]. The influence of plasma-related parameters on the self-organization at the initial stage can be analyzed by the rate equation model which was described in detail elsewhere [7]. In short,

the densities of nanoclusters consisting of a small number of atoms are calculated by the set of rate equations

$$\frac{\partial \eta_i}{\partial t} = \Psi_{\text{ext}} + \dot{\eta}_{i.1} + \dot{\eta}_{i.2} + \dot{\eta}_{i.3} \tag{1}$$

where Ψ_{ext} is the external flux of particles (i.e., ions) to the surface, and $\dot{\eta}_{i.1}$, $\dot{\eta}_{i.2}$, and $\dot{\eta}_{i.3}$ are the rates of density variation of nanoclusters consisting of i atoms due to collisions, evaporation, and adatom attachment, respectively [7]. These processes strongly depend on the surface temperature T and activation energies (typically, the rate of evaporation is described as $v_e = v_0 \exp(-\varepsilon_b/kT)$, the rate of adatom diffusion as $\upsilon_d = \lambda\, v_0 \exp(-\varepsilon_d/kT)$, where λ is the lattice constant, ε_b is the surface evaporation energy, and ε_d is the surface diffusion activation energy, see details in [7,31]). As indicated above, the surface temperature and surface diffusion activation energy are the main parameters (we do not consider the presence of lattice defects and impurities) that influence the kinetics of surface diffusion. The temperature is determined by the energy balance on the surface and is strongly affected by the ion flux and bias. The change in the surface diffusion activation energy of the adsorbed particle, caused by the presence of electric field on the surface, can be estimated as $W_e = |\partial E/\partial r|\lambda\tilde{p}$, where E is the electric field, and $\tilde{p}$ is the dipole moment of the adatom. We use here an absolute value for $\partial E/\partial r$, since the particle with a dipole moment always takes energy from the electric field irrespective of the sign of $\partial E/\partial r$, due to the dipole moment re-orientation in the electric field. Thus, both parameters (temperature and surface diffusion activation energy) are controlled by the plasma environment. Now we will investigate the effect of these two parameters on the self-organizational processes and system behavior.

The results of the numerical simulations are shown in Figs. 1 and 2. Here one can see that small variations (from 0.55 to 0.67 eV) in the surface diffusion activation energy cause a strong change in the distribution function (Fig. 1) and density-time dependence (Fig. 2) of nanoclusters on the surface. The graphs demonstrate that the small change in the activation energy (caused by a 10 % change in the surface bias) can be used to control self-organization processes on plasma-exposed surfaces.

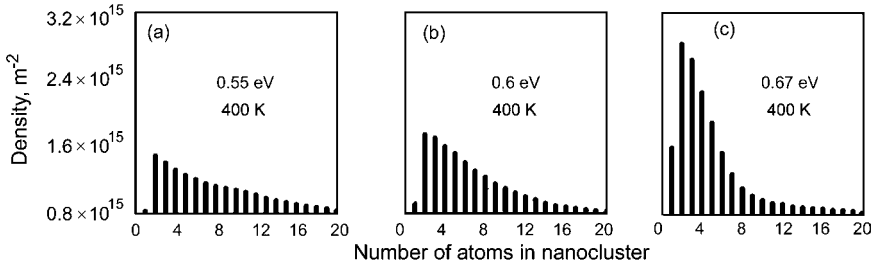

Fig. 1 Nanocluster distribution function with surface diffusion activation energy as a parameter for 0.55 eV (a), 0.6 eV (b), and 0.67 eV (c). The surface temperature is 400 K.

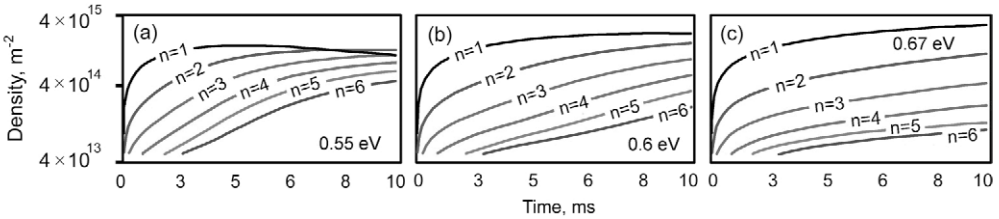

Fig. 2 Dependence of surface density of nanoclusters on time with surface diffusion activation energy as a parameter for 0.55 eV (a), 0.6 eV (b), and 0.67 eV (c). The size of nanocluster (number of atoms n they consist of) is indicated on curves. The surface temperature is 400 K.

CRYSTALLIZATION AND SELF-ASSEMBLY ON PLASMA-EXPOSED SURFACES

Now we consider the next stage of the nanostructure formation, namely, the stage of separate growth of the nanostructures, when they are large enough (include at least several hundreds of atoms) for crystallization, but small enough that they do not interact with neighboring structures (due to relatively large distances between them). At this stage, the processes that determine the shaping and crystallization will play the main role; in this case, the use of the plasma environment becomes particularly important due to the increased energy of ions extracted from the plasma [32–35], which ensures nanostructure crystallization during the growth.

Let us consider the characteristic surface diffusion factor under conditions of localized ion heating $v_\tau = \tau/\tau_C$, where adatom diffusion time (time of adatom residence in one lattice site) at equilibrium surface temperature T is $\tau = 1/v_e$, where τ_C is the adatom diffusion time at increased (via local ion heating) temperature T_C, lattice oscillation frequency $v_0 = 2kT/h$, and lattice oscillation time $\tau_0 = 1/v_0 = h/(2kT)$; here, h is Planck's constant. Thus, the characteristic surface diffusion factor under conditions of local ion heating is

$$v_\tau = \tau / \tau_C = \exp\left[\frac{e\varepsilon_d}{kT}\left(\frac{\delta T}{T_C}\right)\right] \tag{2}$$

where the local temperature is $\delta T = \varepsilon_i e/(kn)$, ε_i is the ion energy, and $T_C = T + \delta T$. Then, the total time of adatom incorporation into nanostructures is $\tau_{C.t} = \sum_1^{n_C} \tau_{C.i}$, where the number of sites on the surface of a nanostructure as a function of the total number of atoms n in the nanostructure is $n_C = \sqrt{8}(3n)^{2/3}$ for a pyramidal QD, and $\tau_{C.i}$ is the adatom diffusion time in i-*th* site at temperature T_C.

The model was used to estimate the rate of adatom diffusion over the surface of a QD. These estimates show that the rate of surface diffusion of an adatom on the QD surface after deposition as an ion is 2.5 … 1000 times higher than after neutral atom deposition. The results are plotted in Fig. 3. The graphs show that the substrate bias and surface diffusion activation energy strongly influence the specific surface diffusion factor, and thus strongly influence the QD crystallization by facilitating surface diffusion about the substrate (Fig. 4a).

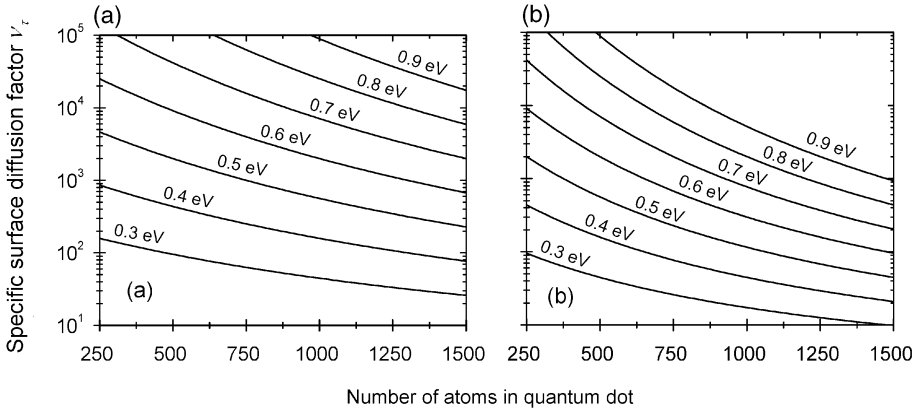

Fig. 3 Dependence of specific surface diffusion factor v_τ on the QD size (number of atoms constituting the QD), with surface diffusion activation energy as a parameter. Surface temperature is 600 K, substrate bias 100 V (a) and 50 V (b).

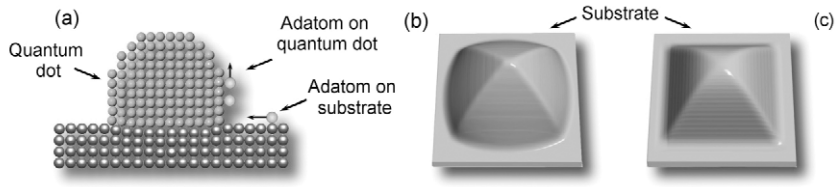

Fig. 4 Scheme of adatom diffusion on QD and surface (a); simulated shapes of Ge QD for substrate bias 50 V (b) and 100 V (c).

In Figs. 4b and 4c, we show the shapes of the self-assembled QDs formed at two different values of surface bias (i.e., at different ion energies) which were simulated by the kinetic Monte Carlo (KMC) technique [36]. It is clearly seen from these figures that the equilibrium shape is better faceted at higher ion energies, which promotes better diffusion about the QD surface under conditions of the localized ion heating. A change of the surface bias voltage within quite realistic limits (50 and 100 V) leads to the noticeable changes in the QD shape.

SELF-ORGANIZATION IN LARGE NANOSTRUCTURE ARRAYS

Now we will consider the specifics of self-organization on plasma-exposed surfaces at the third stage of the nanoarray formation, when a strong interaction (via adatom field and also via the electric field) between the nanostructures is present. At this stage, the adatom diffusion about the substrate surface plays the main role [31,37]. We concentrate mainly on QDs, but other nanostructures can also exhibit self-organized behavior, for example, carbon nanowalls [38].

Let us first consider the experimental results of the QD array formation on plasma-exposed substrates [20,22,39]. The three consecutive scanning electron microscopy (SEM) micrographs are shown in Fig. 5. In Fig. 6, we show the dependence of the mean radius of QDs as a function of time (a) obtained by processing the photographs, and the mean number of QDs in array (b). The upper curve in Fig. 6a shows the experimental results; the lower curve is the theoretically predicted dependence $d = k \cdot t^{1/3}$ which the QDs should follow in the independent growth case. One can see from these graphs that the estimated QD diameter is 25 nm at t = 120 min; the experiment shows 29–30 nm.

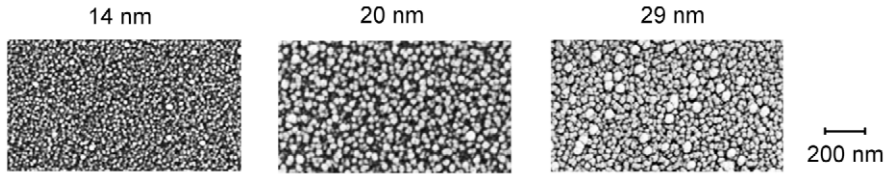

Fig. 5 Development of SiC QD array in a plasma-based process. The mean size of the QDs is indicated above the photos. (Courtesy of S. Xu, Q. Cheng, and K. Ostrikov, unpublished.)

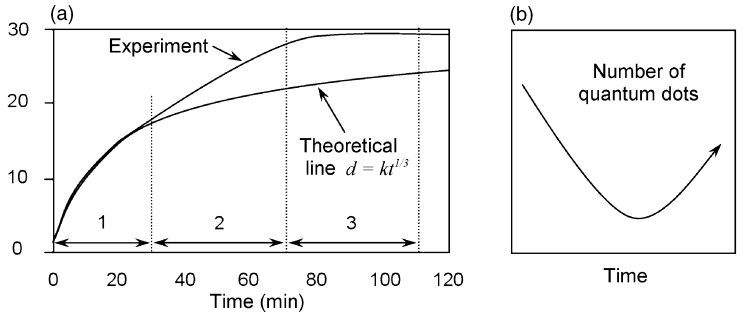

Fig. 6 Dependence of mean QD radius (a) and number of QDs (b) on time.

From these facts, we can make the following conclusions. Firstly, the total number of QDs changes during the growth (Fig. 6b); then, between 40 and 80 min the mean radius increases above the "mass-conserving" value. This means that the number of QDs decreases (in 1.7…2.5 times) between 40 and 80 min; hence, the dissolution and other number-decreasing surface processes take place during the first 80 min of growth. Then, at the final stages the size of QDs does not change (or only decreases slightly). This means that the number of QDs increases. Therefore, the behavior of the QD ensemble (three stages) is as follows: (1) 0–20 min: the number of QDs increases; (2) 20–80 min: the total number of QDs decreases (mostly due to coalescence and dissolution); (3) 80–120 min: the total number of QDs increases (due to nucleation of adatoms on the surface).

Now, let us consider surface diffusion in the presence of an electric field (on biased surfaces). In the process of deposition from a plasma, the QDs acquire electric charge and hence produce an electric field. The total electric field is a sum of the plasma-surface (sheath) component E_λ directed from the surface to the plasma, and the nanostructured component E_S which is present in the vicinity of a single QD and directed to this QD. The plasma effect on the QD formation is caused by these two electric field components, which affect the surface diffusion rate.

Let us estimate the changes in the surface diffusion activation energy caused by the component E_S, taking into account the non-zero polarizability α of the adsorbed particle. In this case, the total dipole moment in the electric field $E(r)$ is $\tilde{P} = \tilde{p} + \alpha E$ (we recall that $\tilde{p}$ is a dipole moment of the adsorbed particle). Thus, the energy taken by the adsorbed particle in one jump across one lattice spacing (λ) is

$$W_e = \frac{\partial E}{\partial r}\left[\tilde{p} + \alpha E(r)\right]\lambda \tag{3}$$

Below, the nondimensional energy will be used

$$\varepsilon_e = \frac{\lambda}{kT}\frac{\partial E}{\partial r}\left[\tilde{p} + \alpha E(r)\right] = \frac{\lambda}{kT}\frac{\partial^2 \varphi}{\partial r^2}\left[\tilde{p} + \alpha E(r)\right] \tag{4}$$

Hence, to obtain ε_e one has to determine the electric field. In a general case, the electric field magnitude is determined by surface electric charge σ through:

$$\varphi = \iint_S d\varphi = \iint_S \frac{\sigma dS}{4\pi\varepsilon_0 r} \tag{5}$$

where S is the QD surface; r is the distance between the surface and the point of potential determination. Surface integral (5) depends on the QD growth shape. There are three main cases: flat QD (the QD height less than radius $h << r_0$); QD in the form of a spherical segment; and a cylindrical QD. For the most typical case of the QD in the form of a spherical segment, the electric field is

$$\varphi = \frac{\sigma}{4\pi\varepsilon_0}\int_0^{\pi/2}\int_0^{2\pi}\frac{r\cdot\bar{r}_0^2\,d\alpha\,d\beta}{\sqrt{\bar{r}_0^2 - 2\bar{r}_0\cos(\alpha)\cos(\beta)+1}} \tag{6}$$

where $\bar{r}_0 = r_0/r$. Some details on calculation of the electric field in nanosized systems can be found in [8,21].

With the electric potential φ found, energy ε_e can be calculated by eq. 4, and the surface diffusion coefficient can be obtained in the form

$$D_S = \lambda^2 \nu_0 e^{-\frac{\varepsilon_d - \varepsilon_e}{kT}} \tag{7}$$

The obtained dependencies suggest that the decreased surface diffusion activation energy results in higher rates of adatoms supply to QDs; besides, this leads to better formation of highly-crystalline QDs and improved crystalline structure. The calculated dependencies of the surface diffusion coefficients on the substrate temperature for various substrate biases and surface diffusion activation energies (Figs. 7 and 8) demonstrate a strong increase with the temperature and a notable decrease with the surface diffusion activation energy.

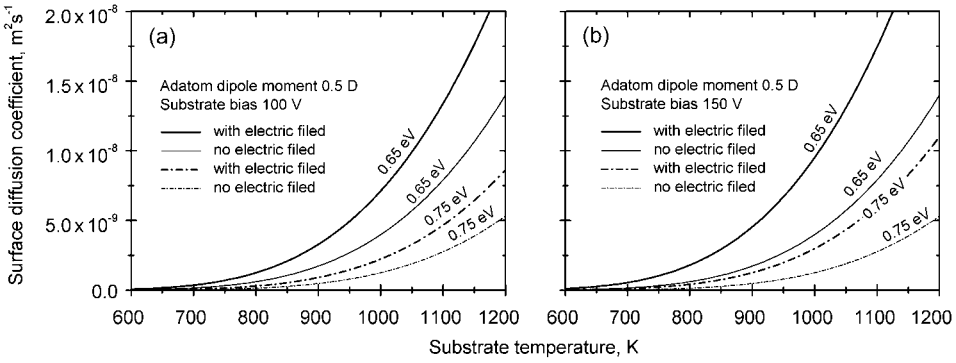

Fig. 7 Dependence of the surface diffusion coefficient on the surface temperature with surface diffusion activation energy in a range of 0.65–0.75 eV as a parameter, adatom dipole moment 0.5 D (1.6×10^{-30} cm), with/without electric field, for substrate bias 100 V (a) and 150 V (b).

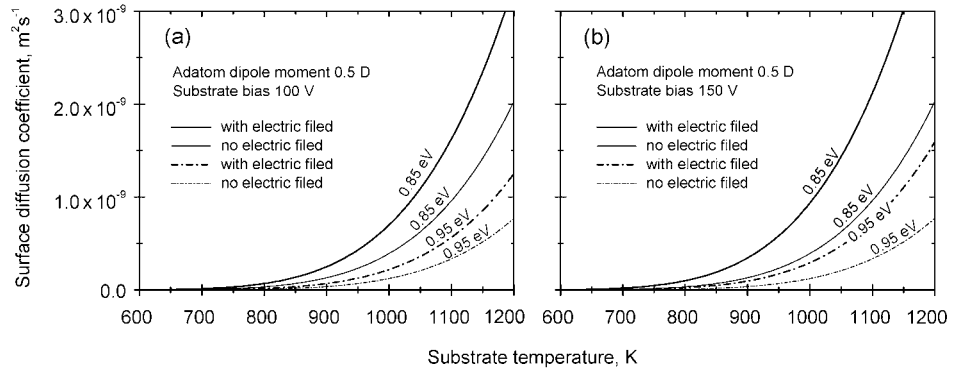

Fig. 8 Dependence of the surface diffusion coefficient on the surface temperature with the surface diffusion activation energy in a range of 0.85 to 0.95 eV as a parameter, adatom dipole moment 0.5 D (1.6×10^{-30} cm), with/without electric field, for substrate bias 100 V (a) and 150 V (b).

Figure 9 illustrates the dependence of the surface diffusion coefficient in the electric field on the surface diffusion activation energy. This dependence covers nearly three orders of magnitude when the surface diffusion activation energy changes from 0.1 to 0.7 eV. This demonstrates a great potential for controlling the diffusion, and hence the self-organization processes on plasma-exposed biased surfaces with the growing QD arrays.

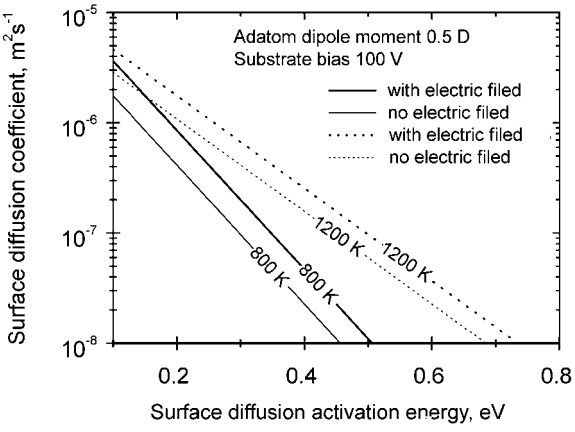

Fig. 9 Dependence of the surface diffusion coefficient in electric field on the surface diffusion activation energy with the surface temperature as a parameter. Adatom dipole moment 0.5 D (1.6×10^{-30} cm), substrate potential 100 V.

As suggested by the above analysis, the surface diffusion coefficient is one of the main factors in the QD array growth and self-organization. QDs in the array grow mainly by the mass supply from the 2D field of adatoms, with the density described by the diffusion equation

$$\frac{\partial \xi}{\partial t} = D_S \left(\frac{\partial^2 \xi}{\partial x^2} + \frac{\partial^2 \xi}{\partial y^2} \right) + \Psi_+ - \Psi_- \tag{8}$$

where ψ_+ and ψ_- are the influx and flux of evaporation from the substrate surface. The two-dimensional adatom field in which the QDs grow causes the spatial self-ordering of the array by redistribution of the adatoms between the QDs.

These processes are illustrated in Fig. 10, where the simulated patterns in (a) and (b), and fragment of SEM micrograph (c) are shown. In the simulated patterns, the QDs marked '1' and '2' on the lower insets change their position, this results in a better (more uniform) pattern shown in (b), as compared with the initial pattern shown in (a). A similar configuration may be noted in the SEM micrograph shown in (c). The experimental details are described elsewhere [40].

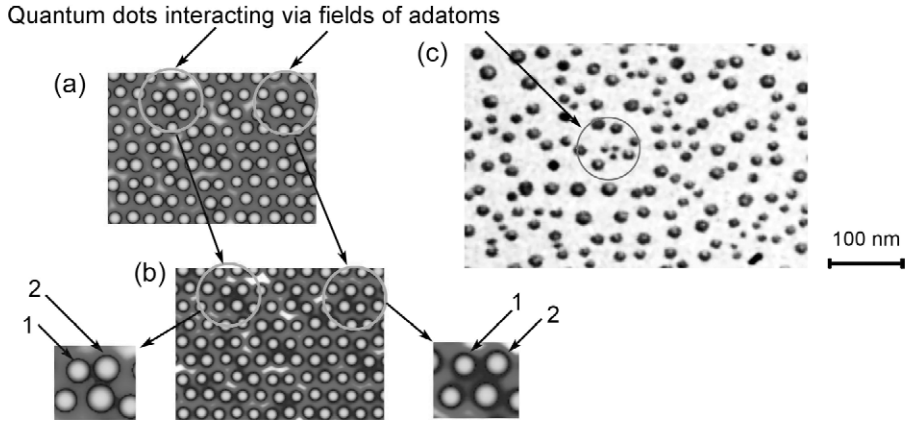

Fig. 10 Self-organization processes in large arrays of SiC QDs. Initial (a) and final (b) simulated patterns, and SEM micrograph (c) of QD pattern on the surface. Pattern (b) is more uniform due to the movement of QDs marked '1' and '2' in the insets (encircled in a and b). SEM image (c) reveals a similar behavior of several QDs (encircled). Photo courtesy of S. Xu, Q. Cheng, and K. Ostrikov, unpublished.

CONCLUSIONS

We have demonstrated the importance of the plasma-related parameters (surface bias and presence of electric fields) and surface conditions for self-assembly, self-organization, and self-ordering processes on solid surfaces. We have shown that the presence of an electric field strongly affects the kinetics of surface diffusion and leads to the crystallization of QDs and better self-organization of large QD arrays. The use of plasma-extracted ions with an increased kinetic energy also results in better crystallization by localized heating of the nanostructures, as well as better reorganization of the QD arrays. Based on this study, we conclude that formation of self-organized nanostructure arrays can be effectively controlled in a plasma environment.

NOTE ADDED IN PROOF

Most recent reports on plasma-controlled self-organized growth of various low-dimensional nanostructures further confirm the effectiveness of various plasma-related controls [41–50].

REFERENCES

1. K. Ostrikov. *Rev. Mod. Phys.* **77**, 489 (2005).
2. M. Keidar, Y. Raitses, A. Knapp, A. M. Waas. *Carbon* **44**, 1022 (2006).
3. A. Okita, Y. Suda, A. Oda, J. Nakamura, A. Ozeki, K. Bhattacharyya, H. Sugawara, Y. Sakai. *Carbon* **45**, 1518 (2007).
4. A. Okita, Y. Suda, A. Ozeki, H. Sugawara, Y. Sakai, A. Oda, J. Nakamura. *J. Appl. Phys.* **99**, 014302 (2006).
5. Z. L. Tsakadze, K. Ostrikov, J. D. Long, S. Xu. *Diam. Relat. Mater.* **13**, 1923 (2004).
6. M. Hiramatsu, K. Shiji, H. Amano, M. Hori. *Appl. Phys. Let.* **84**, 4708 (2004).
7. I. Levchenko, A. E. Rider, K. Ostrikov. *Appl. Phys. Lett.* **90**, 193110 (2007).
8. I. Levchenko, K. Ostrikov. *J. Phys. D: Appl. Phys.* **40**, 2308 (2007).
9. I. Levchenko, K. Ostrikov, J. D. Long, S. Xu. *Appl. Phys. Lett.* **91**, 113115 (2007).
10. I. B. Denysenko, S. Xu, J. D. Long. *J. Appl. Phys* **95**, 2713 (2004).

11. A. Okita, A. Ozeki, Y. Suda, J. Nakamura, A. Oda, K. Bhattacharyya, H. Sugawara, Y. Sakai. *Jpn. J. Appl. Phys.* **45**, 8323 (2006).
12. K. N. Ostrikov, S. Xu, M. Y. Yu. *J. Appl. Phys.* **88**, 2268 (2000).
13. K. Ostrikov, Z. Tsakadze, P. P. Rutkevych, J. D. Long, S. Xu, I. Denysenko. *Contrib. Plasma Phys.* **45**, 514 (2005).
14. F. J. Gordillo-Vázquez, J. M. Albella. *J. Appl. Phys.* **94**, 6085 (2003).
15. U. Cvelbar, B. Markoli, I. Poberaj, A. Zalar, L. Kosec, S. Spaić. *Appl. Surf. Sci.* **253**, 1861 (2006).
16. S. Xu, J. Long, L. Sim, C. H. Diong, K. Ostrikov. *Plasma Process. Polym.* **2**, 373 (2005).
17. F. J. Gordillo-Vázquez, A. Perea, J. A. Chaos, J. Gonzalo, C. N. Afonso. *Appl. Phys. Lett.* **78**, 7 (2001).
18. F. J. Gordillo-Vázquez, A. Perea, A. P. McKiernan, C. N. Afonso. *Appl. Phys. Lett.* **86**, 181501 (2005).
19. K. Ostrikov, A. B. Murphy. *J. Phys. D: Appl. Phys.* **40**, 2223 (2007).
20. C. Mirpuri, S. Xu, J. D. Long, K. Ostrikov. *J. Appl. Phys.* **101**, 024312 (2007).
21. I. Levchenko, K. Ostrikov, E. Tam. *Appl. Phys. Lett.* **89**, 223108 (2006).
22. S. Xu, K. Ostrikov, J. D. Long, H. Y. Huang. *Vacuum* **80**, 621 (2006).
23. I. Levchenko, K. Ostrikov, S. Xu. *Appl. Phys. Lett.* **89**, 033109 (2006).
24. M. Keidar, A. M. Waas. *Nanotechnology* **15**, 1571 (2004).
25. M. Keidar. *J. Phys. D: Appl. Phys.* **40**, 2388 (2007).
26. K. G. Kostov, J. J. Barroso. *IEEE Trans. Plasma Sci.* **34**, 1127 (2006).
27. I. Levchenko, K. Ostrikov, M. Keidar, S. Xu. *J. Appl. Phys.* **98**, 064304 (2005).
28. H. Masuda, K. Yasui, K. Nishio. *Adv. Mater.* **12**, 1031 (2000).
29. U. Cvelbar, M. Mozetic. *J. Phys. D: Appl. Phys.* **40**, 2300 (2007).
30. F. Rosei. *J. Phys. Condens. Matter* **16**, S1373 (2004).
31. I. Levchenko, O. Baranov. *Vacuum* **72**, 205 (2003).
32. K. N. Ostrikov, S. Kumar, H. Sugai. *Phys. Plasmas* **8**, 3490 (2001).
33. I. Levchenko, M. Romanov, M. Keidar. *J. Appl. Phys.* **94**, 1408 (2003).
34. E. Tam, I. Levchenko, K. Ostrikov. *J. Appl. Phys.* **100**, 036104 (2006).
35. I. Levchenko, M. Romanov. *Appl. Phys. Lett.* **85**, 2202 (2004).
36. Z. L. Tsakadze, I. Levchenko, K. Ostrikov, S. Xu. *Carbon* **45**, 2022 (2007).
37. F. Rosei, M. Schunack, Y. Naitoh, P. Jiang, A. Gourdon, E. Laegsgaard, I. Stensgaard, C. Joachim, F. Besenbacher. *Prog. Surf. Sci.* **71**, 95 (2003).
38. I. Levchenko, K. Ostrikov, A. E. Rider, E. Tam, S. V. Vladimirov, S. Xu. *Phys. Plasmas* **14**, 063502 (2007).
39. Q. Cheng, S. Xu, J. Long, K. Ostrikov. *Appl. Phys. Lett.* **90**, 173112 (2007).
40. K. Ostrikov, J. D. Long, P. P. Rutkevych. S. Xu. *Vacuum* **80**, 1126 (2006).
41. I. Levchenko, K. Ostrikov. *Appl. Phys. Lett.* **92**, 063108 (2008).
42. I. Levchenko, K. Ostrikov, A. B. Murphy. *J. Phys. D: Appl. Phys.* **41**, 092001 (2008).
43. K. Ostrikov, I. Levchenko, S. Xu, S. Y. Huang, Q. J. Cheng, J. D. Long, M. Xu. *Thin Solid Films* **516**, 6609 (2008).
44. I. Levchenko, K. Ostrikov. *Nanotechnology* **19**, 335703 (2008).
45. A. E. Rider, I. Levchenko, K. Ostrikov. *Nanotechnology* **19**, 355705 (2008).
46. I. Levchenko, K. Ostrikov, M. Keidar, U. Cvelbar. *J. Phys. D: Appl. Phys.* **41**, 132004 (2008).
47. S. Y. Huang, K. Ostrikov, S. Xu. *J. Appl. Phys.* **104**, 033301 (2008).
48. M. Keidar, I. Levchenko, T. Arbel, M. Alexander, A. M. Waas, K. Ostrikov. *Appl. Phys. Lett.* **92**, 043129 (2008).
49. U. Cvelbar, K. Ostrikov, A. Drenik, M. Mozetic. *Appl. Phys. Lett.* **92**, 133525 (2008).
50. L. Yuan, X. X. Zhong, K. Ostrikov. *Nanotechnology* **19**, 155304 (2008).